

Biotransformation of Sulfonamide Antibiotics in Activated Sludge: Formation of Pterin-Conjugates Leads to Sustained Risk

Stefan Achermann^{1,2}, Valeria Bianco^{1,2}, Cresten B. Mansfeldt¹, Bernadette Vogler¹, Boris A. Kolvenbach³, Philippe F.X. Corvini^{3,4}, Kathrin Fenner^{1,2,5,*}

¹Eawag, Swiss Federal Institute of Aquatic Science and Technology, 8600 Dübendorf, Switzerland.

²Institute of Biogeochemistry and Pollutant Dynamics, ETH Zürich, 8092 Zürich, Switzerland.

³Institute for Ecopreneurship, School of Life Sciences, University of Applied Sciences and Arts Northwestern Switzerland, 4132 Muttenz, Switzerland. ⁴State Key Laboratory for Pollution Control and Resource Reuse, School of the Environment, Nanjing University, Nanjing 210093, PR China.

⁵Department of Chemistry, University of Zürich, 8057 Zürich, Switzerland.

*Corresponding author (email: kathrin.fenner@eawag.ch)

Word count:

Words: 5828

Tables: 2x300 words

Figures: 4x300 words

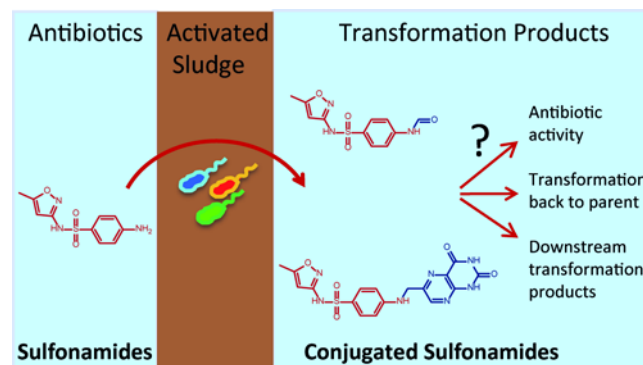
Total: 7628 words

This document is the accepted manuscript version of the following article:
Achermann, S., Bianco, V., Mansfeldt, C. B., Vogler, B., Kolvenbach, B. A., Corvini, P. F. X., & Fenner, K. (2018). Biotransformation of sulfonamide antibiotics in activated sludge: the formation of pterin-conjugates leads to sustained risk. *Environmental Science and Technology*.
<http://doi.org/10.1021/acs.est.7b06716>

1 Abstract

2 The presence of antibiotics in treated wastewater and consequently in surface and ground water
3 resources raises concerns about the formation and spread of antibiotic resistance. Improving removal
4 of antibiotics during wastewater treatment therefore is a prime objective of environmental engineering.
5 Here we obtained a detailed picture of the fate of sulfonamide antibiotics during activated sludge
6 treatment using a combination of analytical methods. We show that pterin-sulfonamide conjugates,
7 which are formed when sulfonamides interact with their target enzyme to inhibit folic acid synthesis,
8 represent a major biotransformation route for sulfonamides in laboratory batch experiments with
9 activated sludge. The same major conjugates were also present in the effluents of nine Swiss
10 wastewater treatment plants. Demonstration of this biotransformation route, which is related to
11 bacterial growth, helps explain seemingly contradictory views on optimal conditions for sulfonamide
12 removal. More importantly, since pterin-sulfonamide conjugates show retained antibiotic activity, our
13 findings suggest that risk from exposure to sulfonamide antibiotics may be less reduced during
14 wastewater treatment than previously assumed. Our results thus further emphasize the inadequacy of
15 focusing on parent compound removal and the importance of investigating biotransformation
16 pathways and removal of bioactivity to properly assess contaminant removal in both engineered and
17 natural systems.

18



19 **Introduction**

20 The widespread presence of antibiotics in the environment raises significant concern because their
21 concentrations are high enough to potentially affect sensitive aquatic ecosystems and their ubiquity
22 may support the propagation of antibiotic resistant genes.¹⁻⁵ Sulfonamides, one of the oldest families
23 of antibiotics, are still widely used as human and veterinary drugs.⁶⁻⁸ They have been detected in
24 various environmental matrices including soil, wastewater, surface water and ground water.^{6,9-11}
25 Particularly for sulfamethoxazole, the sulfonamide antibiotic with the highest reported human
26 consumption, concentrations in the upper ng/L to low µg/L range are frequently detected in municipal
27 wastewater.¹²⁻¹⁷ Biological wastewater treatment plays an important role in reducing the load of
28 chemicals collected by the sewer system prior to discharge to surface waters.¹⁸ Several studies have
29 investigated the sulfonamide removal capacity of biological wastewater treatment systems,¹²⁻¹⁶
30 reporting variable degrees of removal¹⁹ and contradictory results regarding optimal removal
31 conditions.²⁰⁻²⁵

32 Although removal alone has been repeatedly demonstrated to be insufficient in assessing
33 environmental risk,^{26,27} only limited research has been focused on obtaining a clear picture of the fate
34 of sulfonamides during wastewater treatment. Previous investigations have demonstrated that sorption
35 to activated sludge solids and abiotic processes play a minor role and that the majority of observed
36 removal in activated sludge is linked to biotransformation.^{21, 23} However, sulfonamide
37 biotransformation pathways and related transformation product (TP) formation have been little
38 studied. A number of studies focus on the sulfonamide biotransformation capabilities of isolated
39 microbial strains. Several of these studies report the formation of the SMX cleavage product 3A5MI,^{28,}
40 ²⁹ or analogous cleavage products for other sulfonamides.³⁰ One pure culture study performed with
41 ¹⁴C-labeled SMX demonstrated partial mineralization to ¹⁴CO₂.³¹ Another possible biotransformation
42 pathway is related to the original mode of action of sulfonamide antibiotics. The bacteriostatic effect
43 of sulfonamides is based on the competitive inhibition of dihydropteroate synthase (DHPS), a key
44 enzyme involved in intracellular folic acid synthesis. In studies with *Escherichia coli* and, more
45 recently, in different algal species, sulfonamides were shown to act as alternate substrates for the

46 DHPS enzyme, leading to the formation of pterin-sulfonamide conjugates.³²⁻³⁵ Whereas these studies
47 show that certain microorganisms are able to degrade sulfonamides or even use them as carbon source,
48 pure culture results generally cannot be extrapolated to mixed communities.³⁶

49 Limited research has focused on the elucidation of sulfonamide biotransformation in complex
50 activated sludge communities. In a recent study with ¹⁴C labeled SMX, the parent compound was
51 degraded under aerobic as well as anaerobic conditions, but mineralization rates were below 5% under
52 all measured conditions, suggesting that the majority of the spiked micropollutants was still present in
53 the form of unidentified transformation products.²¹ In a different study, a number of SMX metabolites
54 were detected including products potentially formed via acetylation, hydroxylation, nitration,
55 deamination or formylation.³⁷ However, no attempts were made to prioritize the detected TPs and their
56 relative importance remains unclear. Yet, such knowledge is highly desirable to properly assess risk
57 given the fact that sulfonamide metabolites with modifications at the *para*-amino position, including
58 those that are formed when sulfonamides interact with their target enzyme to inhibit folic acid
59 synthesis,³²⁻³⁴ have been shown to still exhibit antibiotic activity.^{38, 39}

60 The objective of this study therefore was to gain a comprehensive view of the transformation
61 pathways and products of sulfonamide antibiotics during wastewater treatment. To this end, we used a
62 combination of two complementary methods, i.e., mass balance analyses with ¹⁴C-labeled
63 sulfonamides and in-depth transformation product screening with high-resolution mass spectrometry
64 of samples from both laboratory batch experiments with activated sludge and field study samples from
65 wastewater treatment plants. Experiments were performed with five non-radiolabeled sulfonamides in
66 parallel (*i.e.*, sulfamethoxazole, sulfadiazine, sulfamethazine, sulfapyridine and sulfathiazole) to
67 evaluate the generalizability of our findings to the entire family of sulfonamide antibiotics.

68 **Methods**

69 **Batch Experiments**

70 For the experiments with radiolabeled sulfonamides, ¹⁴C-SMX (aniline[¹⁴C], Hartmann Analytic) and
71 ¹⁴C-SDZ (2-Pyrimidyl[¹⁴C]-sulfadiazine, Bayer HealthCare) were used. Further details on chemical
72 reference materials are provided in section S1 of the Supporting Information (SI). For all experiments,

73 amber glass bottles (100 mL, Schott) were used as batch reactors. To maintain aerobic conditions, caps
74 with two holes were used as previously described.⁴⁰ After sulfonamide addition, the reactors were
75 placed on a circulating shaker table (160 rpm) for the duration of the experiment and samples were
76 collected at different time points as specified below. Batch reactor experiments with SMX and SDZ,
77 with SMZ, SPY and STZ and with pterin-STZ, respectively, were conducted in three separate
78 campaigns. Therefore, fresh activated sludge was collected three times (21.03.2017 (AS1), 12.06.2017
79 (AS2) and 18.07.2017 (AS3), less than three hours before the experiments were started) from the
80 same aerated nitrifying treatment basin of the same WWTP (ARA Neugut, Dübendorf, Switzerland,
81 details in section S2 in the SI). During all three experimental campaigns, pH values remained in the
82 range between 7.87 and 8.28 at all measured time points. Results from measurements of total
83 suspended solids (TSS), pH and nitrogen species (NH_4^+ , NO_2^- , NO_3^-), and a comprehensive table of
84 all batch experiments including added chemicals, sampling time points and sample volumes is
85 provided in the SI (section S2).

86 **Experiment with Radiolabeled and Non-Labeled SMX and SDZ**

87 Triplicate biotransformation batch reactors with radiolabeled and non-labeled substances were
88 established in parallel, both for SMX and SDZ. Additionally, abiotic controls with autoclaved (30 min
89 at 125 °C) activated sludge and radiolabeled sulfonamides were established in triplicate, and three
90 reactors with only activated sludge added served as non-spiked controls. Biotransformation batch
91 reactors with ¹⁴C-labeled compounds were spiked (40 µL each, 1.53 kBq/µL (SMX) and 1.02 kBq/µL
92 (SDZ) in methanol), resulting in final initial activities of 61.2 kBq (SMX) and 40.8 kBq (SDZ),
93 respectively, corresponding to initial concentrations of 405 µg/L (SMX) and 115 µg/L (SDZ).
94 Reactors with non-labeled sulfonamides were spiked (40 µL each, 250 mg/L, in methanol/water 1:3)
95 to achieve initial concentrations of 250 µg/L (SMX and SDZ). To ensure equal starting conditions in
96 terms of carbon availability, the reactors with non-labeled sulfonamides and the non-spiked controls
97 were amended with 30 µL and 40 µL of methanol, respectively.

98 Samples were collected over 72 hours. The samples were centrifuged at 21500 × g for 10 minutes at
99 room temperature and the supernatant transferred into amber HPLC vials. For the non-radioactive

100 samples, internal standard solution was added (final sample concentration: 24 µg/L, details in section
101 S3). Samples were stored at 4 °C and then analyzed by high-performance liquid chromatography
102 (HPLC) coupled to a high-resolution mass spectrometer (see below for details) within 7 days. For the
103 reactors spiked with radiolabeled sulfonamides, 30 µL of supernatant was transferred into a 6 mL
104 polypropylene vial and mixed with 5 mL of scintillation cocktail (IrgaSafe Plus, Perkin Elmer) for
105 liquid scintillation counting (LSC). In parallel, 750 µL of supernatant were pipetted into amber HPLC
106 vials, stored at 4 °C and then analyzed by HPLC coupled to a diode array detector (DAD) and an LSC
107 detector within 3 days.

108 To analyze the radioactivity adsorbed to or incorporated into the biomass, the compressed solid
109 material resulting from centrifugation was obtained after removal of the remaining supernatant. The
110 cell pellet was washed with NaOH (1 mL, 1M in water) and the washing liquid was collected after
111 another centrifugation run (15 min at 21500 rpm). The entire washing liquid (1 mL) was mixed with
112 scintillation cocktail (5 mL, Hionic Fluor, Perkin Elmer) and analyzed using LSC. The washed cell
113 pellet was stored at -20 °C until analysis in the sample oxidizer as described below. The washing
114 solution contained radioactivity both from ¹⁴C-SA weakly adsorbed to the microbial cells and from
115 remaining aqueous supernatant that was not removed after centrifugation. Since a major fraction of the
116 radioactivity originated from the remaining aqueous fraction and, as we could show for SMX, the
117 fraction attributed to sorption was not exceeding 4% at all investigated time points, the measured
118 radioactivity of the washing solution was not considered in the mass balance analysis (details in
119 section S4 in the SI).

120 **Experiment with Non-Labeled SPY, SMZ, STZ and N4-Acetyl-SMX**

121 Biotransformation experiments with the SAs SMZ, STZ and SPY, and the TP N4-acetyl SMX were
122 run in duplicate. To estimate the degree of sorption and abiotic degradation, SAs were added to
123 duplicate control reactors with autoclaved (121 °C and 103 kPa for 20 min) activated sludge and
124 activated sludge filtrate, respectively. Non-spiked reactors (duplicate) were run to serve as controls in
125 suspect screening. Samples were collected over 72 h and processed similarly to the methods described
126 above. For the biotransformation reactors, 25 µL of each sulfonamide or N4-acetyl-sulfamethoxazole

127 solution (100 mg/L, in methanol/water 1:9) were spiked each into the according batch reactors
128 resulting in a starting concentration in the reactors of 50 µg/L. Samples were centrifuged (5 min at
129 $21130 \times g$), and the supernatant (750 µL) was transferred to amber HPLC vials. After the addition of
130 the internal standard solution, samples were stored for 3–7 days at 4 °C until HPLC-MS/MS analysis.

131 **Experiment with Pterin-STZ**

132 A reference standard for pterin-STZ was custom synthesised by SynphaBase, Switzerland.³⁴ Six batch
133 reactors were filled with activated sludge of which three were spiked with pterin-STZ (25 µL, 100
134 mg/L pterin-STZ, in methanol/water 1:9) and three served as non-spiked controls. Samples were
135 collected over time and centrifuged (10 min at $21130 \times g$), and the supernatant (500 µL) was
136 transferred to amber HPLC vials and stored (for 3–5 days) at 4 °C until LC-MS/MS analysis.

137 **LC-HRMS/MS Analysis**

138 All non-radioactive samples were analyzed by reversed-phase HPLC coupled to a high-resolution
139 tandem mass spectrometer (HRMS/MS) (Q Exactive or Q Exactive Plus, Thermo Fisher Scientific).
140 The separation of the analytes was achieved using a C18 silica-based column (Atlantis-T3, particle
141 size 3 µm, 3.0×150 mm, Waters) at 30 °C. Samples from the experiments with non-labeled SPY,
142 SMZ and STZ were measured using an additional guard cartridge (particle size 3 µm, 3.9×20 mm,
143 Waters) leading to higher retention times (RTs). For all samples, 100 µL of sample was injected onto
144 the column at a flow rate of 300 µL/min. Further analytical details including chromatographic
145 separation and mass spectrometric analysis are provided in section S5 in the SI. For quantification,
146 calibration curves were prepared in nanopure water (Barnstead Nanopure, Thermo Scientific) ranging
147 from 0.2–300 µg/L (SMX and SDZ) and 0.2–75 µg/L (SPY, SMZ, STZ and TPs). To account for
148 compound losses and interferences during LC-HRMS measurements, internal standards were added to
149 all samples, including the calibration samples (details in sections S3 and S5 in the SI). Quantification
150 was performed using Tracefinder EFS 3.2 (Thermo Scientific) for all parent sulfonamides and for
151 transformation products for which reference standards were available. The lowest calibration standards
152 with a meaningful, detectable peak (reasonable peak shape, a minimum of 4 scans per peak and a

153 minimum intensity of 1E04 in Xcalibur Qualbrowser 3.0 (Thermo Scientific)) were regarded as limits
154 of quantification (Table S5.2).

155 **Analysis of Radioactive Residues**

156 Total radioactivity of the samples was assessed using a liquid scintillation counter (Tri-Carb 2800TR,
157 Perkin Elmer). Sample aliquots were mixed with scintillation cocktail prior to the measurements as
158 described above. For analysis of the radioactivity accumulated in the solids, the biomass fractions of
159 the samples were combusted for 1.5 min in a 307 Perkin Elmer Sample Oxidizer. The resulting $^{14}\text{CO}_2$
160 was absorbed by Carbo-Sorb® E (Perkin Elmer) and LSC cocktail (Permafluor® E+, Perkin Elmer)
161 was added. The radioactivity was then assessed by liquid scintillation counting. Radioactive
162 supernatant samples were analyzed using a HPLC 1200 Series (Agilent Technologies) including a
163 diode array detector (DAD) coupled to a subsequent liquid scintillation counter (Ramona Star,
164 Raytest). The DAD signal was recorded at 285 nm (4 nm bandwidth), which is close to the maximum
165 of an absorption peak between 250 and 300 nm in the absorption spectra of both SMX and SDZ.^{41, 42}
166 An identical column and gradient program and identical eluent mixtures and injection volumes for
167 chromatographic separation as described for the LC-HRMS/MS measurements above were used.

168 **Suspect Transformation Product Screening**

169 For the identification of TPs, a suspect screening was performed using Compound Discoverer 2.1
170 (Thermo Scientific) and Xcalibur Qualbrowser 3.0 (Thermo Scientific). Mass lists for the suspect
171 screening were compiled using in silico prediction with the EAWAG pathway prediction system
172 (EAWAG-PPS, <http://eawag-bbd.ethz.ch/predict/>). Additionally, previously reported transformation
173 products and mass shifts of typical biotransformation reactions were considered. Details on the
174 compilation of the suspect TP lists and Compound Discoverer settings are further described in section
175 S6 in the SI.

176 A suspect TP screening was performed for SMX, SDZ, SMZ, STZ, SPY, N4-acetyl-SMX and pterin-
177 STZ. For the N4-acetyl-SMX and the pterin-STZ spike experiments, the suspect TP lists of SMX and
178 STZ, respectively, were used. Measurements from replicate batch reactors were grouped in Compound
179 Discoverer. Further analysis and presentation of results was performed based on mean values from

180 replicate sample values. Detected features matching suspected TP masses were further assessed: Clear
181 differences in time trends between samples and non-spiked controls were ensured, and isotope patterns
182 were compared with calculated isotope patterns of corresponding suspected molecular formulas. For
183 TPs for which a reference standard was available, retention times of suspected TP and reference could
184 be compared. For TPs for which no reference standards were available, MS² spectra were compared
185 with library spectra or interpreted manually. In doing so, the MS² spectra of the TPs were compared
186 with the spectra of the parents or related TPs and with fragments predicted using Mass Frontier 7.0
187 (HighChem). Based on this procedure, confidence levels were assigned to each of the detected TPs as
188 proposed by Schymanski *et al.*, ranging from level 5 “exact mass”, level 4 “unequivocal molecular
189 formula”, level 3 “tentative candidate(s)”, level 2 “probable structure” to level 1 “confirmed
190 structure”.⁴³ Details and MS² spectra are provided in section S7 in the SI.

191 **Wastewater Treatment Plant Samples**

192 From each of nine Swiss WWTPs, three influent and three effluent samples of the biological treatment
193 step were obtained (1-L aliquots of three consecutive 24-h composite samples; flow-proportional
194 sampling except for WWTP3, in which no SMX was detected in influent or effluent, see results) and
195 combined to 72-h composite samples (3 L) in our laboratory. The samples were collected during May
196 and August 2013 and stored at –20 °C until sample preparation. The samples were enriched by solid
197 phase extraction (SPE) and analyzed by HPLC-MS/MS using a modified protocol based on Moschet *et*
198 *al.*⁴⁴ (further details in section S8 in the SI). A suspect TP screening was performed with the 5 SMX
199 TPs N4-acetyl-SMX, PtO-SMX, pterin-SMX, Ac-OH-SMX and N4-formyl-SMX using Tracefinder
200 4.1 (ThermoFisher Scientific) and confidence levels were assigned according to Schymanski *et al.*⁴³
201 Reasonable peak shapes were ensured by visual inspection and isotope patterns were compared with
202 predicted isotope patterns to confirm molecular formulas. Confidence levels assigned in batch
203 experiments were adopted if at least for two fragments (found in batch experiments or library spectra)
204 their extracted ion chromatograms matched the retention times and peak shapes of the corresponding
205 MS¹ extracted chromatograms. To compensate for matrix effects and possible analyte losses during
206 sample preparation and analysis, the detected peak areas were normalized by the peak areas of the

207 internal standard (isotope-labeled SMX). Influent SMX concentrations were quantified using the
208 internal standard method described for the laboratory experiments.

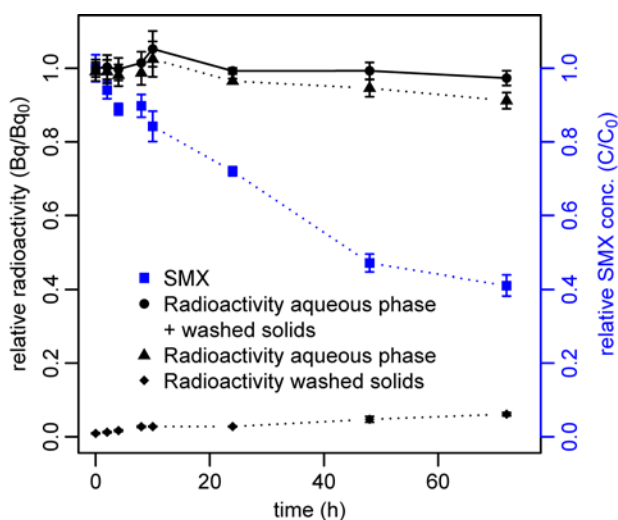
209 **Results**

210 **Biotransformation as Main Removal Mechanism**

211 Analysis of concentration-time series from batch experiments revealed mean removals of 99.3%
212 (sulfathiazole, STZ), 88.7% (sulfapyridine, SPY), 63.8% (sulfadiazine, SDZ), 63.5% (sulfamethazine,
213 SMZ) and 58.9% (sulfamethoxazole, SMX) after 72 hours (from initial concentrations of 405 µg/L
214 (SMX), 115 µg/L (SDZ) and 50 µg/L (SMZ, SPY, STZ)). These removals are comparable to
215 previously reported removals from laboratory studies.^{24, 45} Calculation of TSS-normalized pseudo-first
216 order rate constants resulted in values of 0.083±0.006 (SMX), 0.093±0.009 (SDZ), 0.11±0.01 (SMZ),
217 0.45±0.01 (STZ) and 0.20±0.01 (SPY) L/(g_{TSS}×d) and coefficients of determination (r²) of at least 0.95
218 (see details in section S2 in the SI). In the experiments with ¹⁴C-labeled SMX and SDZ, the sum of the
219 recovered radioactivity in the aqueous and solids fraction accounted for 97.3–105.3% (SMX) and
220 97.2–99.0% (SDZ) of the initially added radioactivity at all time points (Figure 1, section S9 in the
221 Supporting Information (SI)). This indicated that the loss of radioactivity as ¹⁴CO₂ and, therefore, the
222 degree of mineralization must be low, which was consistent with the low fractions of ¹⁴CO₂ recovered
223 from CO₂ traps in preliminary experiments and the fact that we did not find any evidence of significant
224 amounts of dissolved ¹⁴CO₂ accumulated in the batch reactors (details in section S10 in the SI).

225 The fraction of radioactivity recovered from the washed solids (see methods for details on solids
226 washing step) was generally small, but showed an increase over time (72 h) with final maximum
227 values accounting for 6% (SMX) and 3% (SDZ) of the initially spiked radioactivity. Experiments with
228 autoclaved activated sludge further confirmed that only small fractions of the spiked sulfonamides
229 (SAs) were sorbed to the activated sludge and that abiotic transformation was negligible (section S11
230 in the SI). Therefore, the observed declines in parent sulfonamide concentrations can be confidently
231 attributed to biotransformation. Together with the observation that the major part of the radioactivity

232 remained in the aqueous fraction, this indicates that dissolved transformation products must be
233 increasingly present in the supernatant towards later time points.

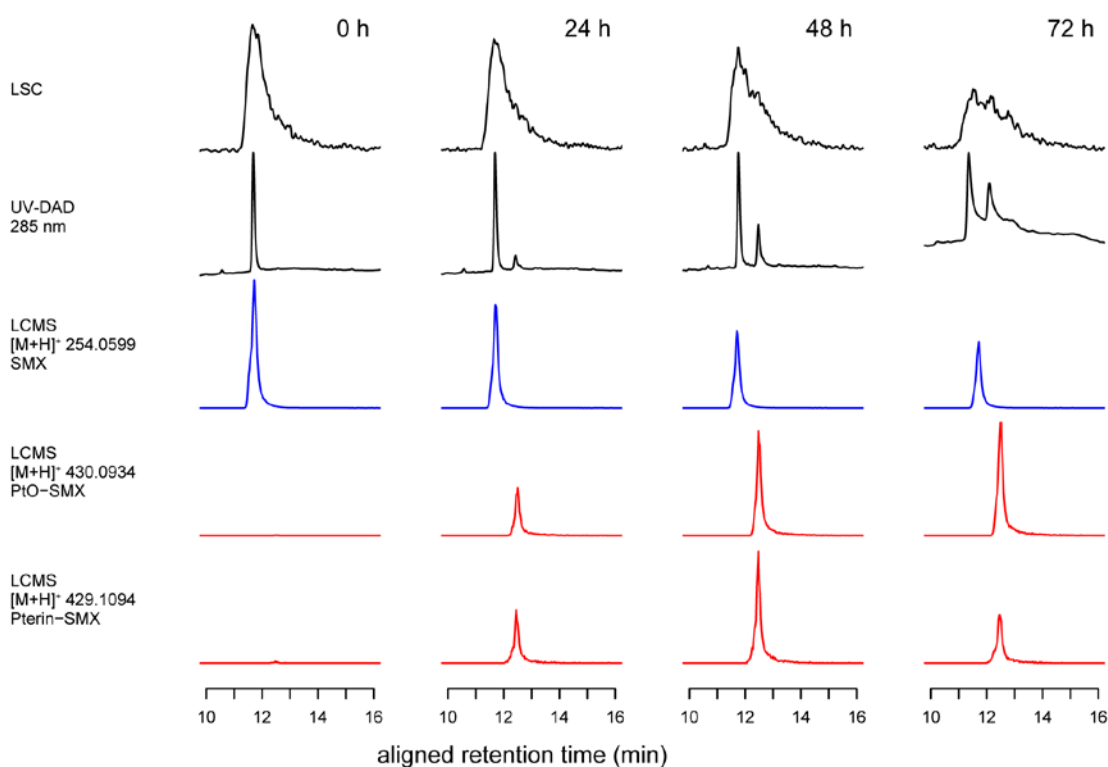


234
235 **Figure 1.** Biotransformation of ¹⁴C-SMX. Radioactivity measured in washed solids, aqueous phase and the sum thereof as
236 fractions of the total radioactivity measured after spiking. Relative concentration of SMX over time is shown in blue. Error bars
237 represent the standard deviation from triplicate reactors.

238

239 Identification of Biotransformation Products

240 To first ensure that all analytes present in the supernatant samples of the ¹⁴C-labeled SMX
241 biotransformation experiment (i.e., SMX and transformation products) could be fully recovered from
242 chromatographic separation, separate radio-scintillating counting of the HPLC effluent was performed
243 and revealed a mean recovery of $100.3 \pm 6.4\%$ for the 0, 24, 28, and 72 hour time points (relative to
244 the total injected radioactivity of a single replicate). The HPLC-UV-DAD and the HPLC-LSC
245 chromatogram both displayed a single dominant SMX peak in the first supernatant sample collected
246 from the biotransformation experiment (Figure 2). In the UV-DAD chromatogram, the intensity of the
247 SMX peak decreased with time, whereas a new peak emerged at a slightly higher retention time (+0.72
248 min). These observations are consistent with broadening and flattening of the SMX peak in the less
249 highly resolved HPLC-LSC chromatogram. The overall peak area in the HPLC-LSC chromatogram
250 (within the retention time window of 10-16 min as shown in Figure 2) showed only a slight decrease
251 ($-12.4 \pm 7.9\%$), suggesting that the major transformation products containing the ¹⁴C-labeled aniline
252 moiety elute at similar retention times as the parent compound.



253

254 **Figure 2.** Chromatograms obtained from different detectors 0, 24, 48 and 72 hours after start of the SMX biotransformation
 255 experiment. LC-MS and LSC signals were aligned with the UV-DAD signal using the peaks corresponding to SMX in the first
 256 sample (0 h). Signal intensities were normalized by maximal intensities over all four time points with the exception of the UV-
 257 DAD signals for which normalization was performed for each sampling point separately (matrix interferences complicated
 258 comparisons of peak intensities and areas). Full chromatograms are shown in section S12 in the SI.

259

260 Suspect transformation product screening of samples from the batch experiments with non-labeled
 261 SMX led to the detection of 11 transformation products (TPs) (Table 1). In Table 1, the TPs are
 262 ordered according to their time-integrated intensities, which were calculated as the sum of measured
 263 peak areas at the different sampling time points. Interestingly, with PtO-SMX (a conjugate of
 264 2,4(1H,3H)-pteridinedione, RT shift: +0.79 min), pterin-SMX (RT shift: +0.77 min) and Ac-OH-SMX
 265 (RT shift: +0.72 min), three of the five TPs with highest time-integrated intensities show similar
 266 retention time shifts relative to the parent as the emerging TP peak observed in the UV-DAD-
 267 chromatogram (Figure 2, section S12 in the SI). This finding suggests that the emerging TP peak in
 268 the UV-DAD-chromatogram is at least partially caused by the emergence of these three TPs.
 269 Moreover, with the exception of 3-amino-5-methylisoxazole (3A5MI), all detected TPs from SMX
 270 show similar RTs as SMX (RT shifts between -0.32 and +1.5 min, Table 1). Since all of these TPs

271 still contain the radiolabeled aniline moiety, their emergence is consistent with the observation that the
 272 overall peak area in the HPLC-LSC chromatogram, despite some broadening and flattening, is only
 273 slightly reduced. This suggests that the majority of SMX might indeed be transformed to the TPs
 274 given in Table 1 (for further discussion of mass balance aspects, see section on biotransformation
 275 pathways).

276 **Table 1. Summary of detected transformation products formed from the five investigated sulfonamides.**

| TP | SMX | | | SDZ | | | SMZ | | | SPY | | | STZ | | |
|---------------------|-------------------|-----------------------------|-------------------------|-------------------|-----------------------------|-------------------------|-------------------|-----------------------------|-------------------------|-------------------|-----------------------------|-------------------------|-------------------|-----------------------------|-------------------------|
| | rank ^a | RT shift [min] ^b | confidence ^c | rank ^a | RT shift [min] ^b | confidence ^c | rank ^a | RT shift [min] ^b | confidence ^c | rank ^a | RT shift [min] ^b | confidence ^c | rank ^a | RT shift [min] ^b | confidence ^c |
| PtO-SA | 1 | 0.8 | 2b | 1 | 1.8 | 2b | 2 | 1.1 | 2b | 4 | 1.5 | 3 | 1 | 1.5 | 3 |
| pterin-SA | 2 | 0.8 | 2b | 6 | 1.8 | 2b | 5 | 1.0 | 2b | 7 | 1.2 | 3 | 4 | 1.4 | 1 |
| N4-formyl-SA | 3 | 1.0 | 2b | 3 | 0.9 | 2b | 4 | 0.1 | 2b | 2 | 0.6 | 2b | 3 | 1.1 | 2b |
| Ac-OH-SA | 5 | 0.8 | 3 | 2 | 1.3 | 3 | 1 | 1.1 | 3 | 1 | 1.3 | 3 | 2 | 1.2 | 3 |
| SA + O ^d | 4 | -0.3 | 3 | 4 | -0.8 | 4 | 6 | -0.5 | 4 | 3 | -3.1 | 4 | | | |
| pterin-SA + H2O | 7 | 0.4 | 3 | 8 | 1.5 | 3 | | | | | | | | | |
| N4-acetyl-SA | 8 | 1.5 | 1 | 5 | 1.8 | 1 | 3 | 0.9 | 1 | 5 | 1.3 | 1 | | | |
| dihydropterin-SA | 9 | 0.6 | 2b | | | | | | | | | | | | |
| pterin-SA + O | 10 | 1.1 | 4 | 7 | 2.2 | 4 | | | | | | | | | |
| SA + C3H2O3 | 11 | 0.4 | 4 | | | | | | | 6 | 0.2 | 4 | | | |
| 3A5MI | 6 | -4.1 | 1 | | | | | | | | | | | | |
| 2A46DP ^e | | | | | | | 7 | -5.1 | 2b | | | | | | |

277 ^aFor each parent SA, TPs are ranked according to time-integrated intensities across all samples. ^bRT shift indicates the
 278 difference in retention time between transformation product and parent SA. ^cConfidence levels according to Schymanski *et al.*⁴³
 279 are assigned to all TPs (details in methods section and section S7 in the SI). ^dFor SMX+O, the molecular structure of N4-
 280 hydroxy-SMX was proposed (details in section S7 in the SI). ^e2-amino-4,6-dimethyl-pyrimidine.

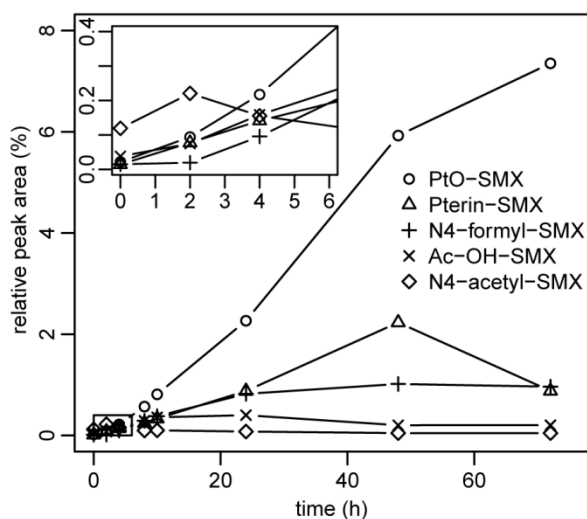
281 HPLC-DAD-LSC chromatograms and recovered radioactive fractions from suspended solids and
 282 aqueous fractions of the SDZ biotransformation experiments confirmed the findings for SMX
 283 described above (section S9 in the SI). Similar to SMX, we observed a broadening and flattening of
 284 the sole LSC-peak present, and collection of the HPLC effluent and separate radio-scintillation
 285 counting again confirmed that all radioactivity could be recovered from the column (mean recovery
 286 for one replicate and time points 0, 24, 48, 72 h: 104.3 ± 3.9 %). Also, a decrease of the parent SDZ
 287 peak was observed in the UV-DAD chromatogram. All eight SDZ-TPs detected in the suspect
 288 screening (Table 1) corresponded to changes in molecular structure that were already observed for
 289 SMX. Furthermore, also for SMZ, SPY and STZ, similar product spectra as for SMX and SDZ were
 290 observed (Table 1). In particular, the TPs PtO-SA, Ac-OH-SA and formyl-SA were consistently

291 observed to rank amongst the five TPs with the highest time-integrated intensities for all five
292 sulfonamides studied.

293 Across all five sulfonamides, PtO-SA was the intensity-wise most dominant TP (i.e., it ranked first for
294 three out of the five sulfonamides (SMX, SDZ and STZ) and had the lowest overall rank sum across
295 all five sulfonamides). PtO-sulfonamides represent a modified pterin-sulfonamide and can presumably
296 be formed by hydrolysis of the latter at position 2 of the pterin condensed ring structure (see
297 discussion below). In our experiments, pterin-SAs were detected for all five investigated
298 sulfonamides. The formation of pterin-SA via dihydropterin-SA has been described previously^{32, 34, 35}
299 and is related to the actual mode of action of sulfonamides as antibacterial agents. Sulfonamides not
300 only act as competitive inhibitors of dihydropteroate synthase but can also act as alternative substrates
301 leading to the formation of pterin-sulfonamide conjugates for which retained antibacterial activity has
302 recently been reported.³⁸ Whereas this process has been described for pure cultures of bacteria and
303 phytoplankton species, its potential significance in activated sludge has not been recognized so far.

304 **Biotransformation Pathways**

305 To obtain more information about the actual biotransformation pathways, we analyzed area-time
306 trends of the detected TPs as presented in Figure 3 for SMX and in section S13 of the SI for SDZ,
307 SPY, STZ and SMZ. For SMX, we observed that the TPs PtO-SMX, pterin-SMX and SMX+O, which
308 we tentatively identified as N4-hydroxy-SMX (confidence level 3 according to Schymanski *et al.*,⁴³
309 see Table 1 and details in section S7 in the SI), show a strong immediate increase upon incubation,
310 whereas N4-formyl-SMX was formed in larger amounts only later in the experiment. Similarly, the
311 N4-formyl TPs of the other sulfonamides also showed a pattern of delayed or slower increase (see
312 section S13), potentially indicating an indirect formation via other TPs.

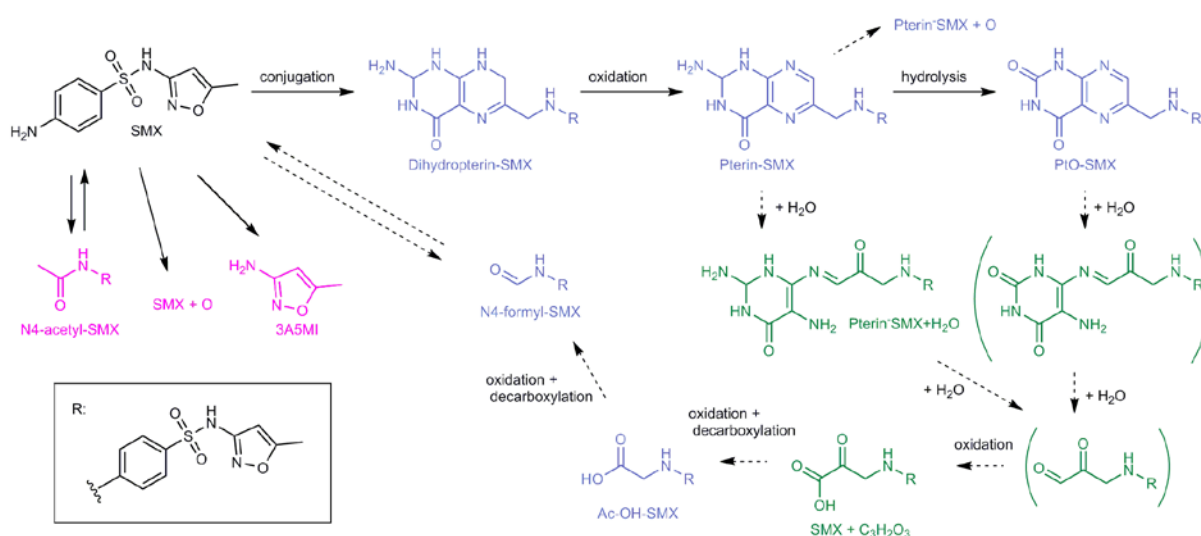


313

314 **Figure 3.** Time trends of transformation products of SMX. Peak areas of selected TPs are shown as percentage of the SMX
 315 peak area in the first sample after spiking. Area-time trends for the remaining TPs detected for SMX and TPs formed from the
 316 other investigated SAs are shown in section S13 in the SI.

317 To investigate the pterin-related biotransformation pathway further, we performed an experiment in
 318 which we directly spiked pterin-STZ to activated sludge. Compared to TP formation in STZ spike
 319 experiments, the observed peak areas of PtO-STZ, Ac-OH-STZ and formyl-STZ were clearly higher
 320 (in the case of PtO-STZ by more than one order of magnitude), which could not be explained by the
 321 minor amounts (approx. 5%) of STZ parent compound present as impurity in the pterin-STZ standard
 322 (Figure S13.6 in the SI). This experiment revealed that not only PtO-STZ was formed from pterin-
 323 STZ, but also Ac-OH-STZ and formyl-STZ. Based on these results we developed a tentative,
 324 generalized pathway for the formation of PtO-SA, Ac-OH-SA and formyl-SA from pterin-SA as
 325 shown in Figure 4. The biotransformation of pterins to 2,4(1H,3H)-pteridinediones (here called PtOs)
 326 has earlier been observed in the context of folic acid biodegradation and can be catalyzed by the
 327 enzyme pterin deaminase.^{46, 47} Although N4-formyl-SA and Ac-OH-SA TPs could theoretically also
 328 be formed directly from the parent sulfonamides, our results suggest that they are rather formed as part
 329 of the pterin-conjugate pathway, involving a series of hydrolysis, oxidation and decarboxylation
 330 reactions acting on either the pterin-SA or the PtO-SA as depicted in Figure 4. For SMX and SPY, a
 331 TP with the mass of the possible intermediate SA+C₃H₂O₃ was additionally detected, and for SMX
 332 and SDZ, a TP with the mass corresponding to pterin-SA+H₂O was found, both lending additional
 333 support to the suggested pterin-conjugate pathway. Additionally, other potentially pterin-related TP

334 peaks were detected corresponding to molecular formulas of pterin-SA+O. Detailed structural analyses
 335 of these TPs were complicated by the detected low peak areas and, hence, not further pursued. In
 336 addition to the pterin-conjugate pathway-related TPs, we also observed the previously described
 337 formation of N4-acetyl-SAs.³⁷ Separate biotransformation experiments with a direct spike of acetyl-
 338 SMX confirmed rapid back-transformation to SMX,¹² suggesting that SMX and acetyl-SMX are
 339 reversibly converted into each other (details in section S14 in the SI). Additionally, for SMX and
 340 SMZ, products resulting from the cleavage of the sulfonamide bridge were observed, namely 3A5MI
 341 and 2-amino-4,6-dimethyl-pyrimidine.



343 **Figure 4.** Proposed biotransformation pathway exemplified for SMX. As confirmed for STZ, PtO-SMX, Ac-OH-SMX and N4-
 344 formyl-SMX are suggested to form via pterin-SMX and the detected intermediate dihydropterin-SMX (blue). TPs corresponding
 345 to masses of pterin-SMX+H₂O and SMX+C₃H₂O₃ were detected but low peak areas did not allow for structure elucidation and
 346 the exact pathway to Ac-OH-SMX and N4-formyl-SMX remains speculative (green). N4-acetyl-SMX, 3A5MI and a TP with the
 347 mass SMX+O may form directly from SMX (pink).

348

349 We could quantify the concentrations of the N4-acetyl metabolites, the cleavage product 3A5MI and
 350 pterin-STZ based on mass spectrometric data. However, together they only accounted for less than
 351 five percent of the removed SMX at all time points. Lacking authentic standards, no accurate
 352 quantification was possible for the other TPs. To obtain an approximate assessment of the mass
 353 balance over the course of the experiment, we estimated relative ionization efficiencies for the
 354 remaining TPs (section S15 in SI) based on structural similarity to those TPs for which authentic
 355 standards were available. Based on authentic standards, the ionization efficiency of pterin-STZ was
 356 found to be one order of magnitude lower than that of STZ (i.e., ratio of instrument response factors of

357 pterin-STZ over STZ: 0.1). Assuming that PtO-SAs exhibit similar ionization efficiencies as the
358 structurally similar pterin-SAs, PtO-SA emerged as the TP that contributed most to the overall mass
359 balance for all sulfonamides. Whereas the mass balance for SMX itself was closed when accounting
360 for all observed TPs (Figure S15.1), some of the other sulfonamides, particularly SPY and STZ,
361 revealed a lack of explainable mass loss, notably at later time points (Figures S15.2-5). This loss
362 suggests that we might still lack a complete representation of later generation TPs formed out of the
363 initial pterin-SA adducts. Although extrapolation of ionization efficiencies involves large
364 uncertainties,^{48, 49} and the calculated mass balances should therefore be interpreted with caution, they
365 lead to strikingly similar conclusions as the results from the ¹⁴C-SMX experiments. In the UV-DAD
366 chromatogram, one dominant TP peak was emerging with a similar retention time shift relative to
367 SMX as the pterin-related TPs PtO-SMX, Ac-OH-SMX and pterin-SMX detected by LC-HRMS.
368 Furthermore, the majority of the radioactivity eluted close to SMX and the above-mentioned TPs.
369 DAD-UV chromatograms and the LSC-chromatograms thus support the dominance of the pterin-
370 conjugate pathway in the biotransformation of sulfonamides.

371 **Detection of Pterin-Sulfonamides in WWTPs Effluents**

372 By applying a suspect TP screening to effluent samples collected from nine Swiss WWTPs, the
373 presence of pterin-conjugate pathway-related sulfonamide TPs could be confirmed. In Table 2, peak
374 areas of TPs and effluent SMX are displayed as fractions of the influent SMX peak area (all peak areas
375 were normalized using internal standards, quantified SMX influent concentrations were between 70
376 and 870 ng/L except for one WWTP where no detectable SMX concentrations were found). For seven
377 out of the nine WWTPs, SMX peak areas showed a decline between 34% and 62% from influent to
378 effluent. In one WWTP (WWTP5), an increase in SMX of 66% between influent and effluent was
379 observed. This can be explained by the large relative peak area of influent N4-acetyl-SMX, which is
380 known to be transformed back to SMX in WWTPs.¹² In the effluent samples, peaks corresponding to
381 pterin-SMX or PtO-SMX were found for seven WWTPs, and in eight WWTP effluents peaks
382 corresponding to Ac-OH-SMX and N4-formyl-SMX were detected. Only in two cases (Ac-OH-SMX
383 in WWTP1 and PtO-SMX in WWTP6) higher or similar TP peak areas were found in influent samples
384 compared to effluent samples. Reassuringly, we found no TP peaks in the effluent of the only WWTP

385 in which no SMX or N4-acetyl-SMX was detected in the influent (WWTP3). Effluent TP peaks
 386 displayed peak areas that were roughly one to two orders of magnitude lower than the influent SMX
 387 peak areas (e.g., $PtO_{\text{effluent}}/SMX_{\text{influent}}$: $13.7 \pm 8.5\%$). However, because of the previously discussed
 388 rather low ionization efficiencies, relatively small pterin-SA peak areas can represent significant
 389 amounts of pterin-SAs. Therefore, the results presented in Table 2 do not only provide evidence for
 390 the formation of pterin-SAs during activated sludge treatment in full-scale WWTPs, but show that the
 391 released pterin-conjugate pathway-related TPs potentially represent major fractions of the
 392 biotransformed SMX. Finally, the diversity of operational and design parameters of the nine WWTPs
 393 (see section S16 in SI for details) suggests that the formation of pterin-SAs is of general relevance and
 394 not limited to the activated sludge used in our biotransformation experiments.

395 **Table 2. Transformation products from SMX detected in wastewater treatment plant effluents.**

| | lvl ^a | WWTP1 | | WWTP2 | | WWTP3 | | WWTP4 | | WWTP5 | | WWTP6 | | WWTP7 | | WWTP8 | | WWTP9 | |
|---------------|------------------|------------------|------------------|-------|-----|-------|-----|-------|-----|-------|-----|-------|-----|-------|-----|-------|-----|-------|-----|
| | | inf ^b | eff ^c | inf | eff | inf | eff | inf | eff | inf | eff | inf | eff | inf | eff | inf | eff | inf | eff |
| SMX | 1 | 100 | 54 | 100 | 38 | nd | nd | 100 | 65 | 100 | 166 | 100 | 38 | 100 | 66 | 100 | 47 | 100 | 59 |
| N4-acetyl-SMX | 1 | 85 | 3 | 59 | 11 | nd | nd | 88 | nd | 559 | 131 | 43 | nd | 112 | nd | 111 | 2 | 165 | 24 |
| pterin-SMX | 2b | nd | 10 | nd | 1 | nd | nd | nd | 1 | nd | 4 | nd | nd | nd | nd | nd | nd | nd | 7 |
| PtO-SMX | 2b | 7 | 23 | 5 | 10 | nd | nd | nd | 5 | nd | 25 | 7 | 7 | nd | 7 | nd | nd | nd | 19 |
| Ac-OH-SMX | 4 | 5 | 3 | nd | 18 | nd | nd | nd | 19 | nd | 92 | nd | 12 | nd | 12 | nd | 3 | nd | 5 |
| N4-formyl-SMX | 2b | nd | 1 | nd | 5 | nd | nd | nd | 3 | nd | 10 | nd | 8 | nd | 4 | nd | 24 | nd | 4 |

396 TP and effluent SMX peak areas are presented as fractions of the peak areas of influent SMX in the respective WWTPs. In
 397 WWTP3 no SMX or SMX TPs were detected in influent or effluent. nd: not detected. ^alevel indicates confidence level of detected
 398 TP structure according to Schymanski *et al.*⁴³ ^bindicates influent. ^cindicates effluent.

399 Implications

400 We demonstrate the significance of the biotransformation of sulfonamides through the pterin-
 401 conjugate pathway and the formation of a suite of derivative transformation products in both batch
 402 biotransformation studies with activated sludge and in municipal wastewater treatment plants.
 403 Although sulfonamides have been previously reported to act as alternate substrates for DHPS and form
 404 pterin-SA conjugates,³² this is the first report of the dominant contribution of this transformation
 405 pathway during wastewater treatment.

406 The relevance of these findings is highlighted by a number of studies that have demonstrated the
 407 potential of dihydropterin- and pterin-SAs to occupy the active site of the DHPS enzyme,^{32, 38, 50} and to
 408 exhibit antibacterial activity by inhibition of the DHPS enzyme.³⁸ In a recent study, dihydropterin-STZ

409 was even used as lead structure to develop novel antibacterial agents based on the replacement of
410 dihydropterin with a quinoxaline moiety.⁵¹ In addition to sulfonamide conjugates, other transformation
411 products of SMX modified at the N4-group, including N4-nitro-SMX and N4-hydroxy-SMX (here
412 tentatively detected and denoted as SMX+O), have been shown to exhibit similar or even higher
413 antibacterial activity than SMX.³⁹ Although no potency information is currently available for the
414 major transformation product PtO-SA, it is a pterin-related conjugate and may demonstrate similar
415 antibacterial activities. Additionally, according to our results, only small fractions of sulfonamides
416 were cleaved at the sulfonamide bridge resulting in transformation products with an undisputable loss
417 of antibiotic activity.³⁹ The fact that N4-acetyl-SMX was demonstrated here and by others^{12, 52, 53} to be
418 readily back-transformed to parent SMX in different environments thus further raises the question of
419 the potential of other pterin-conjugate pathway products such as PtO-SAs, N4-formyl-SA or Ac-OH-
420 SA to be transformed back to the parent sulfonamide in the environment. Taken together our results
421 suggest that although activated sludge treatment in WWTPs reduces the load of parent sulfonamides to
422 the environment, it may well lead to the formation and environmental release of sulfonamide
423 transformation products with similar potential to exert antibiotic activity as the parent compounds.

424 More generally, our results emphasize the claim that quantification of removal of antibiotics alone is
425 insufficient and that transformation products and pathways must be elucidated thoroughly to
426 understand and evaluate the risks related with the usage and subsequent release of antibiotics to the
427 environment. The same point has previously been underscored for other water treatment processes
428 (e.g., aqueous ozonation⁵⁴) and for other classes of biologically active micropollutants (e.g., steroid
429 hormones, for which a variety of transformation reactions has been shown to lead to only minor
430 structural modifications and hence transformation products with retained or even strongly enhanced
431 endocrine-disrupting activities,^{26, 55} or pesticide active ingredients²⁷). Unfortunately, this point is still
432 often ignored in practice. Bioassays that allow measuring relevant endpoints such as antibiotic activity
433 in complex matrices and hence enable an effect-driven approach in transformation product analysis
434 may support consideration of transformation products in future studies.^{56, 57}

435 Finally, our findings are also highly relevant in that they provide a potential explanation of seemingly
436 contradictory findings on optimal conditions for sulfonamide removal in WWTPs. In a number of
437 studies, an association of sulfonamide removal with the addition of readily available carbon sources or
438 measures of heterotrophic activity was found.^{20-24, 58} Yet, others provide evidence suggesting an
439 involvement of ammonia oxidizing microorganisms,^{25, 59} such as correlation of SMX removal with
440 nitrifying activity in an enriched culture of ammonia oxidizing bacteria.²⁵ In turn, this latter finding
441 stands in contradiction with the fact that sulfonamide degradation was mostly insensitive to inhibition
442 of the nitrifiers in batch experiments with activated sludge.⁴⁵ Our results offer a new view on these
443 discussions in that they demonstrate that sulfonamide biotransformation in activated sludge
444 communities is apparently to a large extent related to their interference with folic acid synthesis.
445 Because this pathway is integral to cellular production and maintenance, one can expect sulfonamide
446 biotransformation to pterin-SAs to correlate with bacterial growth. This in turn explains why both
447 nitrifier enrichment cultures and pure heterotrophic cultures both fed with their respective growth
448 substrates, i.e., ammonium or different carbon sources, respectively, show enhanced sulfonamide
449 removal. Sulfonamide biotransformation has also been observed to occur readily under a number of
450 conditions differing from those prevailing in aerated bioreactor experiments with activated sludge. For
451 instance, sulfonamide removal has also been observed under anaerobic^{21, 58, 60} and anoxic^{21, 61}
452 conditions, in microbial communities from river sediments⁵² and river biofilms,⁸ and by different algal
453 species.³⁵ Based on our results, the observed ubiquitous trait of sulfonamide biotransformation in
454 microbial communities becomes a logical consequence of the transformation of sulfonamides through
455 the pterin-conjugate pathway.

456

457 **Acknowledgements**

458 We thank Dr. Hans Peter E. Kohler, Dr. Adriano Joss, Dr. David R. Johnson und Dr. Michael A.
459 Stravs (Eawag) for fruitful discussions and Kevin Kroll (University of Applied Sciences and Arts
460 Northwestern Switzerland) for his help in the radioisotope laboratory. We thank the operators and the
461 staff of the WWTP ARA Neugut for providing activated sludge. We acknowledge financial support
462 from the European Research Council under the European Union's Seventh Framework Programme
463 (ERC grant agreement no. 614768, PRODuCTS) and from the Swiss National Science Foundation
464 (grant agreement no. 310030L_160332). Dr. Anze Zupanic (Eawag) and Dr. Richard E. Lee (St. Jude
465 Children's Research Hospital, Memphis, USA) are acknowledged for helpful comments on the
466 manuscript.

467

468 **Supporting Information**

469 Information on chemical reference compounds; details on biotransformation experiments; analytical
470 details; listing of parameters used for the suspect transformation product screening; structure
471 elucidation of transformation products by analysis of MS² fragmentation spectra; mass spectra;
472 additional results of biotransformation and control experiments and analysis of WWTP samples;
473 estimation of mass balances.

474

475

476 **References**

- 477 1. Kümmerer, K., Antibiotics in the aquatic environment--a review--part I. *Chemosphere* **2009**,
478 75, 417-434.
- 479 2. Michael, I.; Rizzo, L.; McArdell, C. S.; Manaia, C. M.; Merlin, C.; Schwartz, T.; Dagot, C.; Fatta-
480 Kassinos, D., Urban wastewater treatment plants as hotspots for the release of antibiotics in
481 the environment: A review. *Water Res.* **2013**, 47, 957-995.
- 482 3. Kümmerer, K., Antibiotics in the aquatic environment--a review--part II. *Chemosphere* **2009**,
483 75, 435-441.
- 484 4. de Voogt, P.; Janex-Habibi, M. L.; Sacher, F.; Puijker, L.; Mons, M., Development of a common
485 priority list of pharmaceuticals relevant for the water cycle. *Water Sci. Technol.* **2009**, 59, 39-
486 46.
- 487 5. Grung, M.; Kallqvist, T.; Sakshaug, S.; Skurtveit, S.; Thomas, K. V., Environmental assessment
488 of Norwegian priority pharmaceuticals based on the EMEA guideline. *Ecotoxicol. Environ. Saf.*
489 **2008**, 71, 328-340.
- 490 6. Johnson, A. C.; Keller, V.; Dumont, E.; Sumpter, J. P., Assessing the concentrations and risks of
491 toxicity from the antibiotics ciprofloxacin, sulfamethoxazole, trimethoprim and erythromycin
492 in European rivers. *Sci. Total Environ.* **2015**, 511, 747-755.
- 493 7. Hruska, K.; Franek, M., Sulfonamides in the environment: a review and a case report. *Vet.*
494 *Med. Czech.* **2012**, 57, 1-35.
- 495 8. Vila-Costa, M.; Gioia, R.; Acena, J.; Perez, S.; Casamayor, E. O.; Dachs, J., Degradation of
496 sulfonamides as a microbial resistance mechanism. *Water Res.* **2017**, 115, 309-317.
- 497 9. Straub, J. O., Aquatic Environmental Risk Assessment for Human Use of the Old Antibiotic
498 Sulfamethoxazole in Europe. *Environ. Toxicol. Chem.* **2016**, 35, 767-779.
- 499 10. Stoob, K.; Singer, H. P.; Mueller, S. R.; Schwarzenbach, R. P.; Stamm, C. H., Dissipation and
500 transport of veterinary sulfonamide antibiotics after manure application to grassland in a
501 small catchment. *Environ. Sci. Technol.* **2007**, 41, 7349-7355.
- 502 11. Batt, A. L.; Snow, D. D.; Aga, D. S., Occurrence of sulfonamide antimicrobials in private water
503 wells in Washington County, Idaho, USA. *Chemosphere* **2006**, 64, 1963-1971.
- 504 12. Göbel, A.; Thomsen, A.; McArdell, C. S.; Joss, A.; Giger, W., Occurrence and sorption behavior
505 of sulfonamides, macrolides, and trimethoprim in activated sludge treatment. *Environ. Sci.*
506 *Technol.* **2005**, 39, 3981-3989.
- 507 13. Johnson, A. C.; Jürgens, M. D.; Nakada, N.; Hanamoto, S.; Singer, A. C.; Tanaka, H., Linking
508 changes in antibiotic effluent concentrations to flow, removal and consumption in four
509 different UK sewage treatment plants over four years. *Environ. Pollut.* **2017**, 220, 919-926.
- 510 14. Xu, W. H.; Zhang, G.; Li, X. D.; Zou, S. C.; Li, P.; Hu, Z. H.; Li, J., Occurrence and elimination of
511 antibiotics at four sewage treatment plants in the Pearl River Delta (PRD), South China.
512 *Water Res.* **2007**, 41, 4526-4534.
- 513 15. Carballa, M.; Omil, F.; Lema, J. M.; Llompart, M.; Garcia-Jares, C.; Rodriguez, I.; Gomez, M.;
514 Ternes, T., Behavior of pharmaceuticals, cosmetics and hormones in a sewage treatment
515 plant. *Water Res.* **2004**, 38, 2918-2926.
- 516 16. Singer, A. C.; Järhult, J. D.; Grabic, R.; Khan, G. A.; Lindberg, R. H.; Fedorova, G.; Fick, J.;
517 Bowes, M. J.; Olsen, B.; Soderstrom, H., Intra- and inter-pandemic variations of antiviral,
518 antibiotics and decongestants in wastewater treatment plants and receiving rivers. *PLoS One*
519 **2014**, 9, e108621.
- 520 17. Peng, X.; Wang, Z.; Kuang, W.; Tan, J.; Li, K., A preliminary study on the occurrence and
521 behavior of sulfonamides, ofloxacin and chloramphenicol antimicrobials in wastewaters of
522 two sewage treatment plants in Guangzhou, China. *Sci. Total Environ.* **2006**, 371, 314-322.
- 523 18. Ternes, T.; Joss, A., *Human pharmaceuticals, hormones and fragrances*. IWA publishing:
524 2007.
- 525 19. Onesios, K. M.; Jim, T. Y.; Bouwer, E. J., Biodegradation and removal of pharmaceuticals and
526 personal care products in treatment systems: a review. *Biodegradation* **2009**, 20, 441-466.

- 527 20. Majewsky, M.; Gallé, T.; Yargeau, V.; Fischer, K., Active heterotrophic biomass and sludge
528 retention time (SRT) as determining factors for biodegradation kinetics of pharmaceuticals in
529 activated sludge. *Bioresour. Technol.* **2011**, *102*, 7415-7421.
- 530 21. Alvarino, T.; Nastold, P.; Suarez, S.; Omil, F.; Corvini, P. F.; Bouju, H., Role of
531 biotransformation, sorption and mineralization of ¹⁴C-labelled sulfamethoxazole under
532 different redox conditions. *Sci. Total Environ.* **2016**, *542*, 706-715.
- 533 22. Gauthier, H.; Yargeau, V.; Cooper, D. G., Biodegradation of pharmaceuticals by *Rhodococcus*
534 *rhodochrous* and *Aspergillus niger* by co-metabolism. *Sci. Total Environ.* **2010**, *408*, 1701-
535 1706.
- 536 23. Müller, E.; Schüssler, W.; Horn, H.; Lemmer, H., Aerobic biodegradation of the sulfonamide
537 antibiotic sulfamethoxazole by activated sludge applied as co-substrate and sole carbon and
538 nitrogen source. *Chemosphere* **2013**, *92*, 969-978.
- 539 24. Fernandez-Fontaina, E.; Gomes, I. B.; Aga, D. S.; Omil, F.; Lema, J. M.; Carballa, M.,
540 Biotransformation of pharmaceuticals under nitrification, nitratation and heterotrophic
541 conditions. *Sci. Total Environ.* **2016**, *541*, 1439-1447.
- 542 25. Kassotaki, E.; Buttiglieri, G.; Ferrando-Climent, L.; Rodriguez-Roda, I.; Pijuan, M., Enhanced
543 sulfamethoxazole degradation through ammonia oxidizing bacteria co-metabolism and fate
544 of transformation products. *Water Res.* **2016**, *94*, 111-119.
- 545 26. Cwiertny, D. M.; Snyder, S. A.; Schlenk, D.; Kolodziej, E. P., Environmental Designer Drugs:
546 When Transformation May Not Eliminate Risk. *Environ. Sci. Technol.* **2014**, *48*, 11737-11745.
- 547 27. Fenner, K.; Canonica, S.; Wackett, L. P.; Elsner, M., Evaluating pesticide degradation in the
548 environment: blind spots and emerging opportunities. *Science* **2013**, *341*, 752-758.
- 549 28. Reis, P. J.; Reis, A. C.; Ricken, B.; Kolvenbach, B. A.; Manaia, C. M.; Corvini, P. F.; Nunes, O. C.,
550 Biodegradation of sulfamethoxazole and other sulfonamides by *Achromobacter denitrificans*
551 PR1. *J. Hazard. Mater.* **2014**, *280*, 741-749.
- 552 29. Jiang, B.; Li, A.; Cui, D.; Cai, R.; Ma, F.; Wang, Y., Biodegradation and metabolic pathway of
553 sulfamethoxazole by *Pseudomonas psychrophila* HA-4, a newly isolated cold-adapted
554 sulfamethoxazole-degrading bacterium. *Appl Microbiol Biotechnol* **2014**, *98*, 4671-4681.
- 555 30. Deng, Y.; Mao, Y.; Li, B.; Yang, C.; Zhang, T., Aerobic Degradation of Sulfadiazine by
556 *Arthrobacter* spp.: Kinetics, Pathways, and Genomic Characterization. *Environ. Sci. Technol.*
557 **2016**, *50*, 9566-9575.
- 558 31. Bouju, H.; Ricken, B.; Beffa, T.; Corvini, P. F.; Kolvenbach, B. A., Isolation of bacterial strains
559 capable of sulfamethoxazole mineralization from an acclimated membrane bioreactor. *Appl*
560 *Environ Microbiol* **2012**, *78*, 277-279.
- 561 32. Roland, S.; Ferone, R.; Harvey, R. J.; Styles, V. L.; Morrison, R. W., The characteristics and
562 significance of sulfonamides as substrates for *Escherichia coli* dihydropteroate synthase. *J.*
563 *Biol. Chem.* **1979**, *254*, 10337-10345.
- 564 33. Bock, L.; Miller, G. H.; Schaper, K. J.; Seydel, J. K., Sulfonamide structure-activity relationships
565 in a cell-free system. 2. Proof for the formation of a sulfonamide-containing folate analog. *J.*
566 *Med. Chem.* **1974**, *17*, 23-28.
- 567 34. Richter, M. K.; Focks, A.; Siegfried, B.; Rentsch, D.; Krauss, M.; Schwarzenbach, R. P.;
568 Hollender, J., Identification and dynamic modeling of biomarkers for bacterial uptake and
569 effect of sulfonamide antimicrobials. *Environ. Pollut.* **2013**, *172*, 208-215.
- 570 35. Stravs, M. A.; Pomati, F.; Hollender, J., Exploring micropollutant biotransformation in three
571 freshwater phytoplankton species. *Environ. Sci. Proc. Imp.* **2017**, *19*, 822-832.
- 572 36. Larcher, S.; Yargeau, V., Biodegradation of sulfamethoxazole by individual and mixed
573 bacteria. *Appl. Microbiol. Biotechnol.* **2011**, *91*, 211-218.
- 574 37. Majewsky, M.; Glauner, T.; Horn, H., Systematic suspect screening and identification of
575 sulfonamide antibiotic transformation products in the aquatic environment. *Anal. Bioanal.*
576 *Chem.* **2015**, *407*, 5707-5717.

- 577 38. Zhao, Y.; Shadrack, W. R.; Wallace, M. J.; Wu, Y. N.; Griffith, E. C.; Qi, J. J.; Yun, M. K.; White, S.
578 W.; Lee, R. E., Pterin-sulfa conjugates as dihydropteroate synthase inhibitors and
579 antibacterial agents. *Bioorg. Med. Chem. Lett.* **2016**, *26*, 3950-3954.
- 580 39. Majewsky, M.; Wagner, D.; Delay, M.; Bräse, S.; Yargeau, V.; Horn, H., Antibacterial activity of
581 sulfamethoxazole transformation products (TPs): general relevance for sulfonamide TPs
582 modified at the para position. *Chem. Res. Toxicol.* **2014**, *27*, 1821-1828.
- 583 40. Gulde, R.; Meier, U.; Schymanski, E. L.; Kohler, H. P.; Helbling, D. E.; Derrer, S.; Rentsch, D.;
584 Fenner, K., Systematic Exploration of Biotransformation Reactions of Amine-Containing
585 Micropollutants in Activated Sludge. *Environ. Sci. Technol.* **2016**, *50*, 2908-2920.
- 586 41. Abellan, M. N.; Gimenez, J.; Esplugas, S., Photocatalytic degradation of antibiotics: The case
587 of sulfamethoxazole and trimethoprim. *Catal. Today* **2009**, *144*, 131-136.
- 588 42. Espinosa-Mansilla, A.; Salinas, F.; De Orbe Paya, I., Simultaneous Determination of
589 Sulfadiazine, Doxycycline, Furaltadone and Trimethoprim by Partial Least-Squares
590 Multivariate Calibration. *Anal. Chim. Acta* **1995**, *313*, 103-112.
- 591 43. Schymanski, E. L.; Jeon, J.; Gulde, R.; Fenner, K.; Ruff, M.; Singer, H. P.; Hollender, J.,
592 Identifying small molecules via high resolution mass spectrometry: communicating
593 confidence. *Environ. Sci. Technol.* **2014**, *48*, 2097-2098.
- 594 44. Moschet, C.; Piazzoli, A.; Singer, H.; Hollender, J., Alleviating the Reference Standard
595 Dilemma Using a Systematic Exact Mass Suspect Screening Approach with Liquid
596 Chromatography-High Resolution Mass Spectrometry. *Anal. Chem.* **2013**, *85*, 10312-10320.
- 597 45. Men, Y.; Achermann, S.; Helbling, D. E.; Johnson, D. R.; Fenner, K., Relative contribution of
598 ammonia oxidizing bacteria and other members of nitrifying activated sludge communities to
599 micropollutant biotransformation. *Water Res.* **2016**, *109*, 217-226.
- 600 46. Rappold, H.; Bacher, A., Bacterial degradation of folic acid. *J. Gen. Microbiol.* **1974**, *85*, 283-
601 290.
- 602 47. Jayaraman, A.; Thandeeswaran, M.; Priyadarsini, U.; Sabarathinam, S.; Nawaz, K. A.;
603 Palaniswamy, M., Characterization of unexplored amidohydrolase enzyme-pterin deaminase.
604 *Appl. Microbiol. Biotechnol.* **2016**, *100*, 4779-4789.
- 605 48. Oss, M.; Krueve, A.; Herodes, K.; Leito, I., Electrospray ionization efficiency scale of organic
606 compounds. *Anal. Chem.* **2010**, *82*, 2865-2872.
- 607 49. Cech, N. B.; Enke, C. G., Practical implications of some recent studies in electrospray
608 ionization fundamentals. *Mass Spectrom. Rev.* **2001**, *20*, 362-387.
- 609 50. Yun, M. K.; Wu, Y.; Li, Z.; Zhao, Y.; Waddell, M. B.; Ferreira, A. M.; Lee, R. E.; Bashford, D.;
610 White, S. W., Catalysis and sulfa drug resistance in dihydropteroate synthase. *Science* **2012**,
611 *335*, 1110-1114.
- 612 51. El-Attar, M. A. Z.; Elbayaa, R. Y.; Shaaban, O. G.; Habib, N. S.; Abdel Wahab, A. E.;
613 Abdelwahab, I. A.; El-Hawash, S. A. M., Design, synthesis, antibacterial evaluation and
614 molecular docking studies of some new quinoxaline derivatives targeting dihydropteroate
615 synthase enzyme. *Bioorg. Chem.* **2017**, *76*, 437-448.
- 616 52. Radke, M.; Lauwigi, C.; Heinkele, G.; Mürdter, T. E.; Letzel, M., Fate of the antibiotic
617 sulfamethoxazole and its two major human metabolites in a water sediment test. *Environ.*
618 *Sci. Technol.* **2009**, *43*, 3135-3141.
- 619 53. Förster, M.; Laabs, V.; Lamshoft, M.; Groeneweg, J.; Zühlke, S.; Spitteller, M.; Krauss, M.;
620 Kaupenjohann, M.; Amelung, W., Sequestration of manure-applied sulfadiazine residues in
621 soils. *Environ. Sci. Technol.* **2009**, *43*, 1824-1830.
- 622 54. Dodd, M. C.; Rentsch, D.; Singer, H. P.; Kohler, H. P.; von Gunten, U., Transformation of beta-
623 lactam antibacterial agents during aqueous ozonation: reaction pathways and quantitative
624 bioassay of biologically-active oxidation products. *Environ. Sci. Technol.* **2010**, *44*, 5940-5948.
- 625 55. Qu, S.; Kolodziej, E. P.; Long, S. A.; Gloer, J. B.; Patterson, E. V.; Baltrusaitis, J.; Jones, G. D.;
626 Benchetler, P. V.; Cole, E. A.; Kimbrough, K. C.; Tarnoff, M. D.; Cwiertny, D. M., Product-to-
627 parent reversion of trenbolone: unrecognized risks for endocrine disruption. *Science* **2013**,
628 *342*, 347-351.

- 629 56. Jahnke, A.; Mayer, P.; Schäfer, S.; Witt, G.; Haase, N.; Escher, B. I., Strategies for Transferring
630 Mixtures of Organic Contaminants from Aquatic Environments into Bioassays. *Environ. Sci.*
631 *Technol.* **2016**, *50*, 5424-5431.
- 632 57. Escher, B. I.; Fenner, K., Recent advances in environmental risk assessment of transformation
633 products. *Environ. Sci. Technol.* **2011**, *45*, 3835-3847.
- 634 58. Fan, C. H.; Yang, C. W.; Chang, B. V., Anaerobic degradation of sulfamethoxazole by mixed
635 cultures from swine and sewage sludge. *Environ. Technol.* **2017**,
636 10.1080/09593330.2017.1384510.
- 637 59. Torresi, E.; Fowler, S. J.; Polesel, F.; Bester, K.; Andersen, H. R.; Smets, B. F.; Plosz, B. G.;
638 Christensson, M., Biofilm Thickness Influences Biodiversity in Nitrifying MBBRs-Implications
639 on Micropollutant Removal. *Environ. Sci. Technol.* **2016**, *50*, 9279-9288.
- 640 60. Gonzalez-Gil, L.; Mauricio-Iglesias, M.; Serrano, D.; Lema, J. M.; Carballa, M., Role of
641 methanogenesis on the biotransformation of organic micropollutants during anaerobic
642 digestion. *Sci. Total Environ.* **2017**, *622-623*, 459-466.
- 643 61. Hai, F. I.; Li, X.; Price, W. E.; Nghiem, L. D., Removal of carbamazepine and sulfamethoxazole
644 by MBR under anoxic and aerobic conditions. *Bioresour. Technol.* **2011**, *102*, 10386-10390.

645

646